24th International Conference & Exhibition on Electricity Distribution (CIRED)

12-15 June 2017

Session 3: Operation, control and protection

Evaluation of existing DC protection solutions on an active LVDC distribution network under different fault conditions

ISSN 2515-0855
doi: 10.1049/oap-cired.2017.0673
www.ietdl.org

Dong Wang ✉, *Abdullah Emhemed, Patrick Norman, Graeme Burt*

Department of Electronic & Electrical Engineering, University of Strathclyde, Glasgow, UK
✉ *E-mail: d.wang@strath.ac.uk*

Abstract: Low-voltage direct current (LVDC) distribution is considered as one of the new promising technologies for better integration of distributed generation, and supplying local loads in more efficient way compare to AC systems. However, DC protection is still considered as one of the outstanding challenges that holds back the wide deployment of LVDC in the last mile utility applications. Most of existing DC solutions have been developed for specific applications such as data centres, photovoltaic (PV) systems, electric ships, and traction systems. However, their suitability for providing a good level of protection and safety for an LVDC last mile public network is still not fully understood. Therefore, this study evaluates the performances of a wide number of DC protection solutions that have been proposed for the applications on an active LVDC last mile distribution network with local generation sources (including PVs and battery storages). Based on the findings, recommendations of LVDC protection for resilient operation are presented in the study.

1 Introduction

The requirements for clean energy and more efficient power distribution systems have stimulated the interest in low-voltage direct current (LVDC) distribution network. LVDC distribution systems have already been introduced for powering certain applications such as data centres, information communication systems, electric traction systems, and electric ships. Using DC infrastructure with such applications will eliminate the losses caused by AC to DC conversion for supplying DC loads [1].

However, DC fault protection is still considered as one of the outstanding challenges that hold back the wide deployment of LVDC in the last mile utility applications [2]. Many researches have concluded that traditional low voltage (LV) protection solutions that have been used for existing low-voltage alternating current (LVAC) will require longer time for detecting and clearing DC faults, resulting in the requirement for equipment with higher ratings [3]. For other related DC applications such as high voltage direct current (HVDC) transmission, marine systems, DC microgrids, and data centres, different DC protection solutions have been developed [4–12]. However, the suitability of such solutions for providing a good level of protection and safety for an active LVDC last mile distribution network is still not clear. There is still no real application of LVDC last mile with the lack of mature protection solutions in this field. Therefore, using simulation and detailed models of LVDC and associated power electronics converters, this paper extensively evaluates the performances of different existing DC protection solutions on an LVDC last mile distribution network with local generation sources. The paper outlines the challenges and opportunities for using such existing solutions for LVDC last mile networks.

2 Existing DC protection solutions

Existing non-unit and unit DC protection solutions are discussed as follows.

2.1 Non-unit protection

DC overcurrent protection is a current-based protection that has been widely used in different DC systems. Delta criterions based protection is proposed for meshed HVDC grid comparing the current and voltage measurements of positive pole and negative pole to detect the DC fault [5]. More advanced DC protection solutions have been introduced to improve the selectivity of overcurrent protection. For example, rate of change of current-based protection that is using local measurements to analyse the rate of change of current to detect and locate DC faults [6]. In addition, signal-processing techniques (i.e. fast Fourier transform and wavelet transform) have been used for protecting DC marine systems [7], HVDC [8], and LVDC grids [9]. Moreover, converter coordinated protection has been introduced for protecting DC microgrid using fault tolerant converters and contactors to reconfigure the DC network to ride through DC fault conditions [10].

2.2 Unit protection

With respect to unit protection, DC differential protection has been investigated by many researches for protecting LVDC microgrids. Fast DC differential protection (within 10 μs) can be achieved by using communication links and solid-state circuit breakers [11]. In addition, fast directional-based DC protection (1 ms communication delay + 30 μs) has been proposed for an LVDC last mile distribution network [12].

2.3 DC fault interruption devices

There are main four types of devices that can be used for interrupting DC faults. These include fuses, mechanical breaker such as moulded-case circuit breakers (MCCB) and miniature circuit breaker (MCB), solid-state circuit breakers (SSCB), and hybrid SSCB. Fuse-based technologies have been introduced for protecting solar PV such as Eaton Bussmann series [13]. MCCB and MCB have already been available in the market that are used for protecting DC-powered data centres [14]. The SSCBs use

semiconductor switches such as gate turn-off, insulated gate commutated thyristor, insulated gate bipolar transistor, and metal-oxide-semiconductor field-effect transistor (MOSFET) to obtain the fast fault isolation (in few microseconds [15]). Comparatively, hybrid SSCB consists of the mechanical contactor and semiconductor switches to provide the effective and fast DC fault isolation [16]. SSCBs and hybrid SSCB are not widely used and still at an early stage of development.

3 Evaluation of existing protection technologies for protecting an active LVDC distribution network

This section evaluates the effectiveness of DC overcurrent, differential, directional, and rate of change of current protection solutions for protecting future LVDC distribution networks. A detailed model of LVDC distribution network is developed in PSCAD/EMTDC and used as a test network, and simulation studies are conducted to test the performances of each aforementioned protection on the developed test network. The modelling and simulation works are introduced in the following sections.

3.1 Modelling an active LVDC distribution network

The developed test network is based on the LVDC model established in [2] and shown in Fig. 1. The network is supplied from 11 kV AC source with fault level 156 MVA and $X/R = 5$. The LVDC network is connected to the secondary substation of 11 kV/0.4 kV transformer through two-level voltage source converter (VSC). The VSC provides 750 Vdc (±375 Vdc) with midpoint grounding, which facilitates the detection of ground faults [17]. Two 1 km feeders are modelled with a resistor ($R = 0.164\ \Omega$/km) connected in series with an inductor ($L = 0.24$ mH/km) [2].

The model configurations of the VSCs, battery, and PV with their associated controls are presented by Wang *et al.* [18]. In this paper, an isolated dual active bridge (DAB) DC–DC converter and voltage balancers are used to represent the DC–DC converters. The DAB converter is more flexible for different grounding configurations and has better fault management capability than the basic half bridge DC/DC converter [19]. The converter topology is given in Fig. 2, and the associated close loop control is given in Fig. 3 [19]. The parameters of DAB converter are illustrated in Table 1.

The voltage balancer as presented in Fig. 2 is used with the two-level VSC and the DAB DC–DC converters to ensure DC voltage balance between the poles and the operation of the LVDC

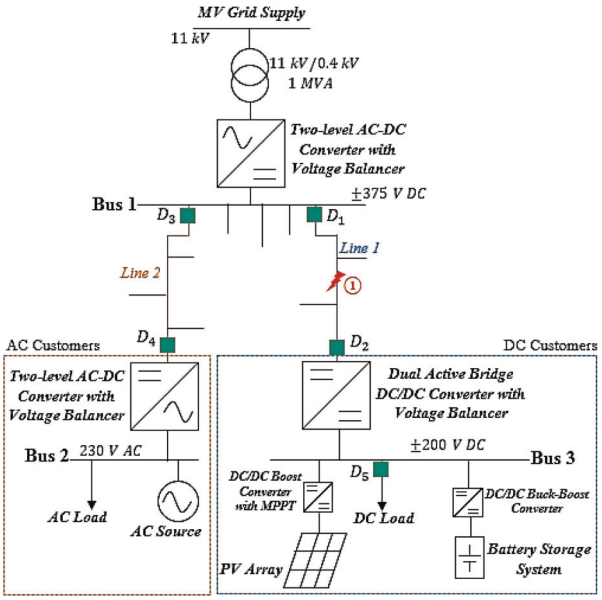

Fig. 1 *LVDC distribution network test model*

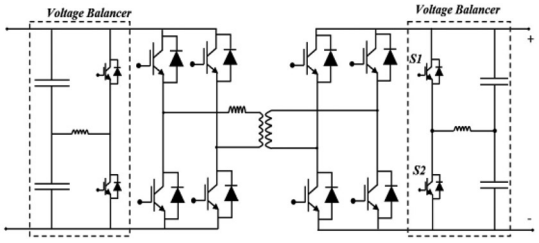

Fig. 2 *Circuit diagram of DAB converter with voltage balancer*

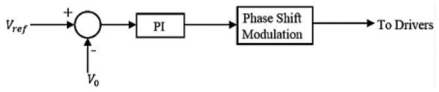

Fig. 3 *Control diagram of DAB [19]*

Table 1 Parameters of dual active bridge converter

	Value
DC capacitor	3300 μF
switching frequency	500 Hz
DC voltage	750 V (± 375 V)/400 V (± 200 V)

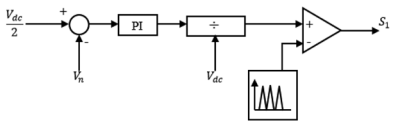

Fig. 4 *Control diagram of voltage balancer [20]*

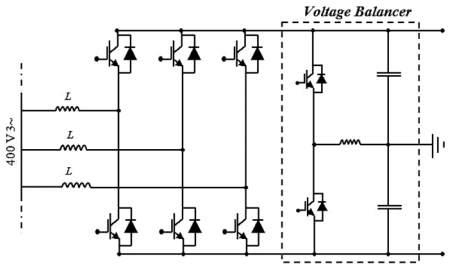

Fig. 5 *Two-level VSC with voltage balancer*

under unbalanced loading conditions. The control of voltage balancer is presented in Fig. 4. The *V*dc/2 is measured and compared to *V*n (voltage of negative pole), and the difference is processed through proportional-integral (PI) and pulse-width modulation (PWM) techniques to generate the required control signals for the balancer (Fig. 5) [20].

3.2 Evaluation of DC protection

In this evaluation, DC pole to pole (P-P) and positive pole to ground (P-G) faults are applied at location 1 (middle of line 1) as shown in Fig. 1, which occur at 1.5 s. The following part will illustrate the performances of DC overcurrent, differential, directional, and rate of change of current-based protection solutions under such fault conditions. In addition, converter impacts on the effectiveness of these protection schemes will be investigated.

3.2.1 DC overcurrent-based protection: Overcurrent protection is modelled as an inverse-time overcurrent relay that is selected with extremely inverse of IEEE Std. C37.112, and

CIRED, Open Access Proc. J., 2017, pp. 1–5

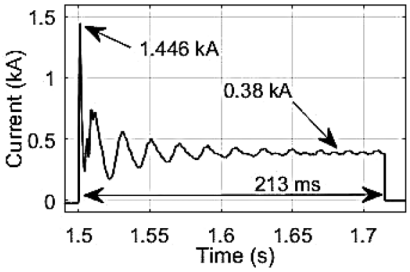

Fig. 6 *Fault current measured at D1 with over current protection during the location 1 P-P fault condition*

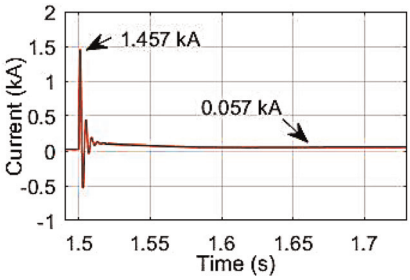

Fig. 7 *Fault current measured at D2 with overcurrent protection during the location 1 P-P fault condition*

threshold setting of D1 and D2 are 1.4 and 1.3 p.u., respectively. The breaker is modelled with 10 ms time delay for arc extinction [21]. During the location 1 P-P fault, D1 overcurrent protection is relatively slow (213 ms) to clear the fault that results in the system experiences the significant transient (1.446 kA) and steady state (0.38 kA) fault currents as presented in Fig. 6, and these lead to the high fault let through energy (FLTE, $\int_0^t I^2 \mathrm{d}t$) (36,800 A^2 s for the cable, 35,000 A^2 s for the grid AC/DC converter). At the D2 side, the steady-state fault current is limited by DAB converter, and only the transient current spike is experienced. The transient and limited steady state fault currents are not enough for the overcurrent protection to operate as illustrated in Fig. 7. In addition, in the positive P-G fault condition, the fault current only has the transient discharge (1.435 kA) as manifested in Fig. 8 that is also not enough for overcurrent protection to operate. This increases the risk of damage to the devices connected to the healthy pole as the operation voltage becomes double as shown in Fig. 9.

3.2.2 DC differential-based protection: Differential protection is modelled following the configuration introduced in [11] with 20% of normal current as the threshold, and solid state circuit breaker is modelled with 1 μs delay [15]. In the location 1 P-P fault condition, fast protection (fault current stops

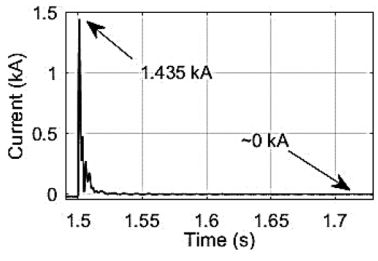

Fig. 8 *Fault current measured at D1 with overcurrent protection during the location 1 positive P-G fault condition*

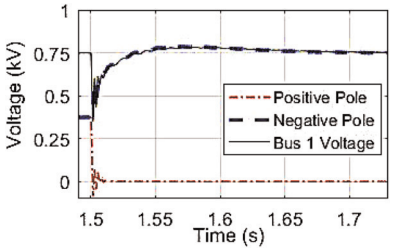

Fig. 9 *Bus one voltage with overcurrent protection during the location 1 P-G fault condition*

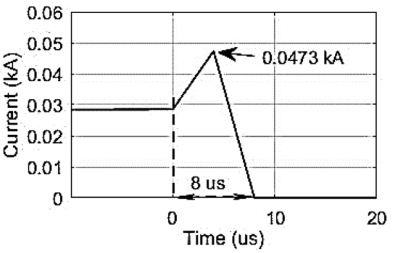

Fig. 10 *Fault current measured at D2 with differential protection during the location 1 P-P fault condition*

increasing in 4 μs) can be achieved that results in the smaller current spike (0.0473 kA) and lower FLTE (only 0.0088 A^2 s for the cable) as shown in Fig. 10. In addition, during the location 1 P-G fault, the voltage of bus 1 can be maintained to the normal voltage level. However, in this test bed, with 20% threshold setting, 12 μs communication delay can cause mal-trips during the external fault conditions. With respect to the high resistive fault detection capability, 20% threshold is capable of detecting 50 Ω fault.

3.2.3 DC directional-based protection: Directional-based protection is configured following the instructions in [12] with the solid-state circuit breakers. Using DC directional protection, fast DC fault protection can be achieved, and the relative current and voltage performances under location 1 P-P and P-G fault conditions are similar as shown in Figs. 10 and 11. However, communication delay is also an issue for directional-based DC protection that could result in the mal-operations. Moreover, high resistive fault detection is a significant issue for directional protection. Fig. 12 shows the current measurement at D1 under location 1 P-G fault. In this test bed, any line 1 P-G faults with resistance higher than 16.7 Ω have the same current direction as the normal operation, which makes directional protection blind.

3.2.4 DC rate of change of current-based protection: Rate of change of current (d*i*/d*t*) based protection is modelled following [6] with solid-state circuit breaker. For example, the threshold

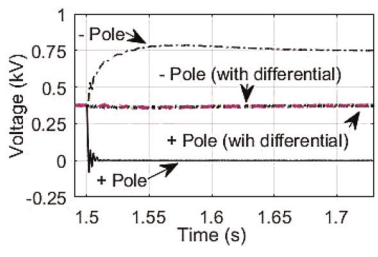

Fig. 11 *Bus one voltage with differential protection during the location 1 P-G fault condition*

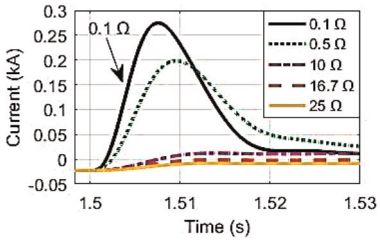

Fig. 12 *Current measurement at D1 under location 1 P-G fault conditions with different fault resistances*

setting for the line 1 protection can be calculated as shown in (1), where, $V_c(0)$ and $i_L(0)$ are voltage and current in the normal operation, R and L are the resistor and inductor of the faulted circuit

$$\frac{\mathrm{d}i}{\mathrm{d}t} = \frac{V_c(o) - i_L(o) \times R}{L} \simeq \frac{V_c(o)}{L} = \frac{750\,\mathrm{V}}{0.00048H} = 1562500\left(\mathrm{A/s}\right) \tag{1}$$

Using this scheme, DC short-circuit fault can be detected and located with high accuracy, and fault can be cleared at the early stage of the current transient. The current and voltage profiles during location 1 P-P and P-G faults are similar as shown in Figs. 10 and 11. However, data acquisition will be a challenge for this scheme. If the measurement misses the transient point, fault detection and location will come with intolerant errors as shown in Fig. 13 (i.e. 0.5 ms measurement delay leads to protection blind). Moreover, using the simplified equation to estimate high resistive fault, errors will be encountered because it neglects the effect of $i_L(0) \times R$ of the original equation. The error can be calculated as depicted in (2). For example, in location 1 P-P fault condition, distance error and fault resistance can be illustrated in Fig. 14, di/dt is very sensitive to fault resistance (i.e. 11 Ω leads to 50% estimation error)

$$\text{Error} = \frac{i_L(\mathrm{o}) \times R}{V_c(\mathrm{o}) - i_L(\mathrm{o}) \times R} \tag{2}$$

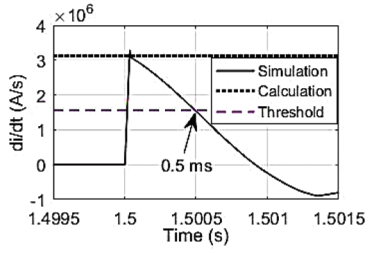

Fig. 13 *Measured and calculated di/dt in the D1 side when P-P fault happens in location 1*

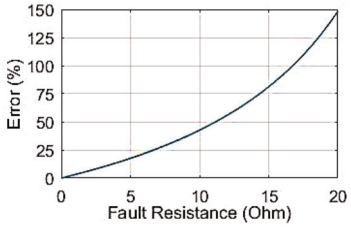

Fig. 14 *di/dt error with fault resistance in the location 1 P-P fault condition*

3.3 Discussion

Mechanical circuit breaker (CB)-based overcurrent (O/C) protection schemes have already been widely used for protecting DC applications. However, their relatively slow performances (i.e. 213 ms) will require the network cables and associated power electronics converters to be designed with higher ratings and larger sizes to withstand fault currents within such duration (i.e. FLTE 35,000 A^2 s for the grid AC/DC converter). In addition, the results also show mechanical CB-based inverse-time graded O/C protection did not operate for DC faults controlled by dual active bridge DC/DC converters. This is because, the fault during the steady state current phase will be limited to a very low value (0.057 kA) which is not enough to trigger the CB.

Comparatively, SSCB-based DC protection solutions (e.g. differential, directional, and rate of change of current) can achieve fast DC fault protection with speed close to 8 µs. This will allow the use of equipment with lower short circuit ratings (0.0088 A^2 s FLTE). However, the cost and losses of SSCB still remain as outstanding issues, and low voltage SSCBs are still at research stages [15]. There is a trade-off between having a cheap mechanical CB-based O/C protection with high cost converters and using fast SSCB-based protection with added losses to the systems.

As for communication-based DC protection solutions, differential protection is more effective than other methods (such as overcurrent, directional, and rate of change of current-based DC protection solutions) for detecting DC faults (especially high resistive faults). For example, 50 Ω fault can be detected and cleared within 10 µs.

In the future, fault tolerant converters (such as modular multilevel converter and dual active bridge converter) are likely to be widely deployed with LVDC distribution systems. Such technologies will allow the use of lower rating power electronic devices with reduced cost [22]. This will require an effective coordination between the converters and downstream DC protection schemes to achieve an enhanced DC fault detection, location, and interruption at low fault level currents.

4 Conclusions

The paper has investigated the effectiveness of existing protection solutions that included DC overcurrent, differential, directional, and rate of change of current-based protection solutions. Currently, in terms of fast speed requirements and high resistive DC fault detection, differential protection with SSCB is the promising solution compare to other methods such as inverse-time graded O/C protection. The challenge with differential protection is the cost where high speed and fidelity communications, intelligent electronic devices, and SSCBs are required. In addition, O/C protection is hard to detect and interrupt the reduced fault currents caused by fault tolerant converters. For future LVDC distribution power systems, when fault tolerant converters are widely used, new protection techniques such as active-based methods will be more attractive to provide the required advanced DC protection. This field will indeed need further research and tests.

5 References

1 Ahmed, T.E., Ahmed, A.M., Osama, A.M.: 'DC microgrids and distribution systems: an overview', *Electr. Power Syst. Res.*, 2015, **119**, pp. 407–417
2 Emhemed, A., Burt, G.: 'An advanced protection scheme for enabling an LVDC last mile distribution network', *IEEE Trans. Smart Grid*, 2014, **5**, (5), pp. 2602–2609
3 Dragicevic, T., Lu, X., Vasquez, J., *et al.*: 'DC microgrids – part II: a review of power architectures, applications, and standardization issues', *IEEE Trans. Power Electron.*, 2016, **31**, (5), pp. 3528–3549
4 Farhadi, M., Mohammed, O.A.: 'Protection of multi-terminal and distributed DC systems: design challenges and techniques', *Electr. Power Syst. Res.*, 2017, **143**, pp. 715–727
5 Marten, A.K., Troitzsch, C., Westermann, D.: 'Non-telecommunication based DC line fault detection methodology for meshed HVDC grids'. 11th IET Int. Conf. on AC and DC Power Transmission, 13 July 2015

6 Meghwanni, A., Srivastava, S., Chakrabarti, S.: 'A non-unit protection scheme for DC microgrid based on local measurements', *IEEE Trans. Power Deliv.*, 2017, **32**, (1), pp. 172–181
7 Christopher, E., Sumner, M., Thomas, D., *et al.*: 'Fault location in a zonal marine power system using active impedance estimation', *IEEE Trans. Ind. Appl.*, 2013, **49**, (2), pp. 860–865
8 Nanayakkara, O., Rajapakse, A., Wachal, R.: 'Travelling-wave-based line fault location in star-connected multiterminal HVDC systems', *IEEE Trans. Power Deliv.*, 2012, **27**, (4), pp. 2286–2294
9 Saleh, K., Hooshyar, A., El-Saadany, E.: 'Hybrid passive-overcurrent relay for detection of faults in low-voltage DC grids', *IEEE Trans. Smart Grid*, 2017, **8**, (3), pp. 1129–1138
10 Cairoli, P., Kondratiev, I., Dougal, R.: 'Coordinated control of the bus tie switches and power supply converters for fault protection in DC microgrids', *IEEE Trans. Power Electron.*, 2013, **28**, (4), pp. 2037–2047
11 Fletcher, S., Norman, P., Fong, K., *et al.*: 'High-speed differential protection for smart DC distribution systems', *IEEE Trans. Smart Grid*, 2014, **5**, (5), pp. 2610–2617
12 Emhemed, A., Fong, K., Fletcher, S., *et al.*: 'Validation of fast and selective protection scheme for an LVDC distribution network', *IEEE Trans. Power Deliv.*, 2017, **32**, (3), pp. 1432–1440
13 Eaton: 'Complete and reliable solar circuit protection', January 2016. Available at: www.eaton.com
14 ABB: 'Technical application papers No. 5 ABB circuit-breakers for direct current application', 12 September 2011. Available: www.abb.com
15 Shen, Z., Miao, Z., Roshandeh, A.: 'Solid state circuit breakers for DC microgrids: current status and future trends'. 2015 IEEE 1st Int. Conf. on DC Microgrids, 9 July 2015
16 Hauer, W., Bartonek, M.: 'A novel low voltage grid protection component for future smart grids'. UPEC 2016, September 2016
17 Karppanen, J., Kaipia, T., Nuutinen, P., *et al.*: 'Effect of voltage level selection on earthing and protection of LVDC distribution systems'. 11th IET Int. Conf. on AC and DC Power Transmission, 13 July 2015
18 Wang, D., Emhemed, A., Burt, G., *et al.*: 'Fault analysis of an active LVDC distribution network for utility applications'. UPEC 2016, September 2016
19 Zhao, B., Song, Q., Liu, W., *et al.*: 'Overview of dual-active-bridge isolated bidirectional DC–DC converter for high-frequency-link power-conversion system', *IEEE Trans. Power Deliv.*, 2014, **29**, (8), pp. 4091–4106
20 Han, B.: 'A half-bridge voltage balancer with new controller for bipolar DC distribution systems', *Energies*, 2016, **9**, (3), p. 182
21 Ma, R., Rong, M., yang, F., *et al.*: 'Investigation on arc behavior during arc motion in air DC circuit breaker', *IEEE Trans. Plasma Sci.*, 2013, **41**, (9), pp. 2551–2560
22 Qi, L., Liang, J.: 'Design issues and practical application challenges of DC shipboard distribution system protection'. Electric Ship Technologies Symp. (ESTS), 16 July 2015